

## STRUCTURAL AND FATIGUE FEATURES OF Ti64 ALLOY AFTER DIFFERENT LASER SHOCK PEENING

A. N. Vshivkov, A. Yu. Iziyomova, E. A. Gachegova, and O. A. Plekhov

UDC 539.421

*To select the optimal treatment mode of Ti64 alloy specimens with a stress concentrator, several laser shock peening (LSP) modes are studied. The effectiveness of the modes was determined by two criteria: indirect, based on the residual stress (RS) profile formed immediately after LSP (the depth of the layer with compressive RS and its maximum value), and direct, based on the number of cycles to failure during fatigue testing of Ti64 alloy flat specimens after hardening by LSP. The most effective LSP mode, which improves the fatigue properties of the specimens with the concentrator of the studied geometry, has been determined. To study the physical RS generation mechanisms, structural studies of the specimens after LSP have been carried out using the Electron Backscatter Diffraction (EBSD) method. The obtained data include the spread of the grain orientation, the average grain misorientation, and the change in the number of defects in the grains under different LSP modes. The results of the microstructure studies correlate with the profiles of the residual stresses caused by LSP.*

**Keywords:** Laser shock peening, residual stress, fatigue, EBSD, crack.

### INTRODUCTION

The exhaustion of constructive ways for increasing the service life of tool parts has led to the creation of new methods for materials treatment to improve their properties. Compared to the traditional surface treatment methods (shot peening, rolling, and laser heat hardening), the laser shock peening (LSP) treatment has a number of advantages: no need for contact between the part and the tool during treatment and no global thermal effect as well as the possibility of local treatment of complex geometry parts and short treatment time. This makes the LSP surface hardening technology for treating parts in the aerospace and energy industries economic and practically competitive. Despite the fact that shock wave generation using high-intensity laser pulses dates back to the early 1960s [1], this technique has not yet received wide industrial application for improving the surface properties of materials. Only in the 90s of the last century, with the development of the technology, it became possible to create safe, compact, and easily controllable high-energy laser systems. The technology is based on modification of the surface layer properties and creation of the residual stress (RS) field. The spatial configuration of the RS field, the magnitude of the maximum compressive RSs, and the depth of the layer in which the compressive RSs are formed play significant roles in the initiation of defects and the development of material damage. At the same time, the main purpose of using LSP as a hardening technology is not only the formation of the RS field to a given depth and with a given geometry, but also the increase of the service life and the improvement of fatigue and strength properties of parts and structures of different geometry, their corrosion resistance, and the restoration of the working components subject to corrosion and fatigue [2–8]. In the field of scientific research, the low-cycle fatigue of the blade AZ80-T6 alloy sample hardened by hot LSP has been studied to date in work [9]. The laser used for hardening had a wavelength of 1064 nm, a characteristic pulse duration of 20 ns,

---

Institute of Continuous Media Mechanics of the Ural Branch of the Russian Academy of Sciences, Perm, Russia, e-mail: vshivkov.a@icmm.ru; fedorova@icmm.ru; gachegova.e@icmm.ru; poa@icmm.ru. Original article submitted December 20, 2023.

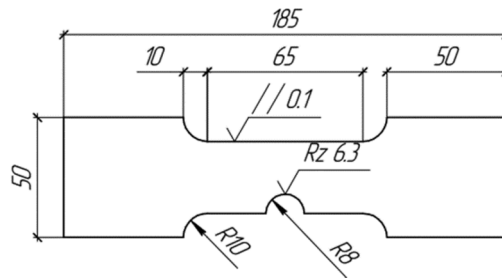


Fig. 1. Geometry of the Ti64 alloy specimens 3 mm thick.

an impact energy of 6 J, a laser spot diameter of 5 mm, and a power density of 1.54 GW/cm<sup>2</sup> [9]. An increase in the fatigue life by 11% with LSP and by 76% with hot LSP (300°C) was found compared to the initial state. Works [10, 11] studied the structures after their laser impact treatment. J. Zhao *et al.* [12] developed a numerical model by the finite element method and analyzed the residual stress intensity to assess the effect of the LSP mode on the crack propagation. The experimental and numerical study of the fatigue crack behavior in the Ti-17 alloy was carried out by R. Sunab *et al.* [13], who determined the conditions for crack retardation and showed that a significant slowdown in the crack growth rate occurred in samples at high RS values, small gap distances during peening, and low applied external loads. The optimal LSP mode of slowing down or stopping the growth of a fatigue crack in an aluminum alloy 2024, including the selection of RS fields by changing the laser treatment power and coating, was discussed by D. C. van Aswegen and C. Polese [14], who took into account the size and position of the hardened area to create a balance between the induced compressive residual stresses and the resulting tensile residual stresses to obtain improved fatigue life and resistance to damage. To investigate the regularities of the fatigue crack growth in materials after LSP, a comprehensive study is required based on modern techniques and developed scientific approaches. Thus, it is important not only to evaluate the configuration of the RS field induced by the laser treatment, but also to carry out mechanical tests, and only after treatment to estimate the effectiveness of the selected treatment mode and determine the optimal laser radiation parameters. The present work aims to create an optimal LSP mode in which not only the structure of the surface layer changes and the RS field with the necessary characteristics is formed (with the compressive RS layer depth in the range of 0.1–1.0 mm and the maximum compressive RS value of at least 600 MPa), but also the fatigue properties of the specimens of the studied geometry are improved after LSP.

## EXPERIMENTAL SETUP FOR LSP IMPLEMENTATION

To study various LSP modes, plane Ti64 ( $\alpha + \beta$ ) alloy specimens 3 mm thick with a round stress concentrator were used. The geometry of the specimens is shown in Fig. 1. The material at the stage of specimen manufacturing was not subjected to additional treatment. The Ti64 alloy is widely used as a structural material for manufacturing various semi-finished products (foils, strips, sheets, plates, forgings, stampings, profiles, pipes, etc.), parts, and structures, including welded ones. They are widely used in aerospace engineering for manufacturing large-sized welded and prefabricated aircraft structures, semi-finished products, and cylinders operating under pressure. The chemical composition of the Ti64 alloy complies with GOST 19807-91.

The LSP treatment system includes a solid state Nd:YAG laser SGR-Extra (Beamtech Optronics Co., Ltd) and a STEP SR50 robotic six-axis manipulator. The laser wavelength is 1064 nm, the maximum pulse repetition frequency is 5 Hz, the maximum pulse energy is 9 J, and the pulse duration is 10 ns. The robotic 6-axis manipulator with a load capacity of 50 kg and a positioning accuracy of 0.25 mm allows automated treatment of specimens of arbitrary geometry. During treatment, the manipulator automatically positions the workpiece in front of the laser beam so that the beam falls normally to its surface; then it instructs the laser machine to generate a pulse using transistor-transistor logic. The laser beam lines are generated using the specialized software based on the three-dimensional model of the

specimen. With appropriate selection of the LSP parameters (the pulse repetition frequency, pulse energy, and laser beam shape), the setup generates the laser radiation energy density in the range 1.11–90 GW/cm<sup>2</sup>.

There are several experimental methods for evaluating the residual stress field, including laboratory X-ray diffraction, neutron diffraction, and synchrotron X-ray diffraction methods [15]. In the present work, the RS depth profile was obtained by drilling holes in flat specimens (according to ASTM E837-13a) and using an MTS3000-Restan automated system for measuring the RSs. This system was used to make simple and accurate measurements by strain gauge hole drilling with a high-speed air turbine (400 000 rpm). The strain gauge with three measuring grids was installed on the surface of the sample in a certain place of which the hole with a diameter of 1–2 mm was drilled. Drilling occurred step by step; at the end of each step, the strain gauge fixed values of the whole deformations obtained after removal of the compressive residual stresses. The measurement error did not exceed 1  $\mu\text{m/m}$ . The data obtained were used to calculate the residual stress profiles by solving the corresponding inverse problem.

Among the advantages of the hole-drilling method are its relative ease of use and availability, no need for special sample preparation, short time to obtain the result, and sufficient accuracy. Among the limitations of the method are the need for the flat sample surface, the possibility of RS measurements only at one point on the surface, the need to select appropriate strain gauge sizes if the sample is sufficiently small, and the possibility of obtaining only two residual stress components. The fatigue properties were investigated on a Bi-00-100 servo-hydraulic testing machine with 100 kN capacity under uniaxial cyclic loading with constant stress amplitude of 111 MPa and cycle asymmetry coefficient  $R = 0.1$ . The crack length was measured by the Direct Current Potential Drop (DCPD) method [16]. The results of data processing are presented in the form of the graphs showing the time dependence of the crack length and the diagrams illustrating the durability of the tested specimens depending on the LSP mode and structure of the material after LSP.

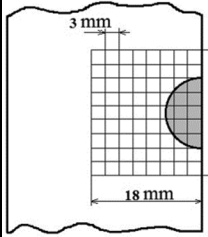
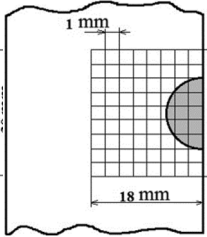
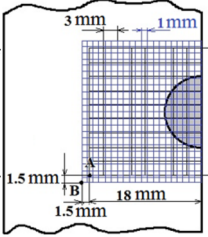
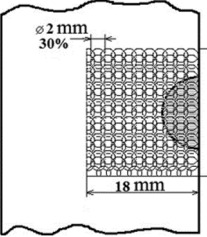
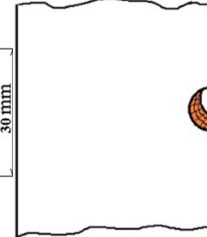
The microstructure of the samples after LSP was studied by the EBSD method for specimens after LSP treatment cut off at half depth. The specimen surfaces were preliminary prepared for metallographic examination by long-term (24 h) vibration polishing with colloidal silica. The data obtained by the EBSD method were mapped using a FEI Quanta 600 FEG SEM equipped with a TSL OIMTM system operating at an accelerated voltage of 20 kV. The high-resolution EBSD analysis was carried out with a scan step of 0.2  $\mu\text{m}$ . To improve the EBSD data accuracy, the grains consisting of two or fewer pixels were automatically removed from the EBSD maps using the grain dilation option in the TSL software.

## SPECIMEN TREATMENT MODES

Five LSP modes were chosen to study the influence of the LSP parameters on the RS profile and the number of loading cycles to failure. The following characteristics were varied in the investigated LSP modes: the laser pulse energy, the shape of the laser pulse imprint on the specimen surface, and the overlap and location of the treated area. Table 2 gives the parameters of the implemented LSP treatment modes. The aluminum foil 80  $\mu\text{m}$  thick was used as an ablation layer.

The LSP treatment according to modes 1–4 was carried out on the planes of the specimens on both sides. Mode 5 assumed treatment only on the round notch. Modes 1 and 2 had the same geometric patterns, but differed in the specific laser power density due to different spot sizes and laser energies. The laser beam imprints on the sample surface were produced butt-to-butt, without any overlap. From the geometric viewpoint, mode 3 is the superposition of modes 1 and 2 with horizontal and vertical shifts of the starting point of the second layer by 1.5 mm. Mode 4 differed from modes 1 and 3 in the shape of the laser beam profile and the presence of an overlap between the beam imprints on the treated surface. The overlap is necessary with a round beam profile in order to avoid the appearance of untreated areas on the material in which undesirable tensile stresses can occur. The maximum treatment time for one specimen surface was 2 min (mode 3), and the minimum time was 0.2 min (mode 2). Mode 5 differed radically from modes 1–4 in the curvilinear area chosen for the LSP treatment in the round notch. Due to the peculiarity of the treated area geometry for mode 5, the laser impact frequency was reduced from 5 Hz to 1 Hz; therefore, the treatment time of a smaller area was 1.25 min.

TABLE 2. Parameters of the LSP Modes for the Flat Ti64 Alloy Samples with a Round Notch

Mode	1	2	3	4	5
					
Energy, J	1	5	2 (1)	2	1
Area, mm	Square 1 × 1	Square 3 × 3	Square 3 × 3 (1 × 1)	Circle Ø2	Square 1 × 1
Power density, GW/cm <sup>2</sup>	10	5.56	2.22 (10)	6.37	10
Overlap, %	0	0	0	30	0
Time, s	108	12	120	56	75

## RESULTS OF RS MEASUREMENTS FOR THE FLAT Ti64 ALLOY SAMPLES

The first criterion for evaluating the effectiveness of the LSP modes is the RS profile formed as a result of LSP treatment. The measurements were carried out near the circular notch, at a distance of 3 mm from its top. Figure 2 shows the measured RS profiles on the specimens after LSP treatment using the five modes described above. The results showed that when implementing mode 1, the maximum value of compressive residual stresses was observed on the sample surface equal to 600 MPa for both components, and the depth of the compressive residual stress layer was 0.9 mm. When implementing mode 2, judging by the obtained RS profile, the field was not sufficiently uniform (the dependences of the components  $\sigma_x$  and  $\sigma_y$  on the layer depth were different). The value of the  $x$  component of the maximum compressive stresses was 400 MPa, and for the  $y$  component it was 200 MPa. The maximum values of the compressive RS components were observed at the same depths of 0.3 mm. After specimen treatment using mode 3, a compressive RS field was formed with a maximum value of 600 MPa at a depth of about 0.1 mm; the depth of the entire layer with compressive RS was 0.6 mm. The optimal mode in terms of the compressive residual stress magnitude and the treated layer depth was mode 4. As a result of its application, it became possible to form the compressive residual stress layer up to 0.8 mm deep, while the maximum values of both compressive residual stress components were 800 MPa near the sample surface. For mode 5, the laser impact was on the notch edge, where it was not possible to use the hole-drilling method due to its limitations. The data obtained at a point similar to the measurement point in modes 1–4 did not give a correct idea of the residual stress field formed in the concentrator in mode 5. Thus, according to the obtained RS profiles, the most effective is mode 4.

## FATIGUE TEST RESULTS

To estimate the number of cycles to failure, 21 samples were studied. The diagram illustrating the dependence of the fatigue life on the LSP mode is shown in Fig. 3. The average number of cycles before the specimen destruction without treatment is  $129995 \pm 22132$ ; after treatment in mode 1, it is  $142570 \pm 7335$ ,  $98719 \pm 12374$  in mode 2,  $115995 \pm 20068$  in mode 3, and  $133286 \pm 45973$  in mode 4. Among the four tested samples processed in mode 5, two samples were not brought to failure with the number of operating cycles 1060127 and 3108610, and two other specimens failed not in the stress concentrator zone, but in the grip area with the number of operating cycles 1007076 and 1159345, respectively.

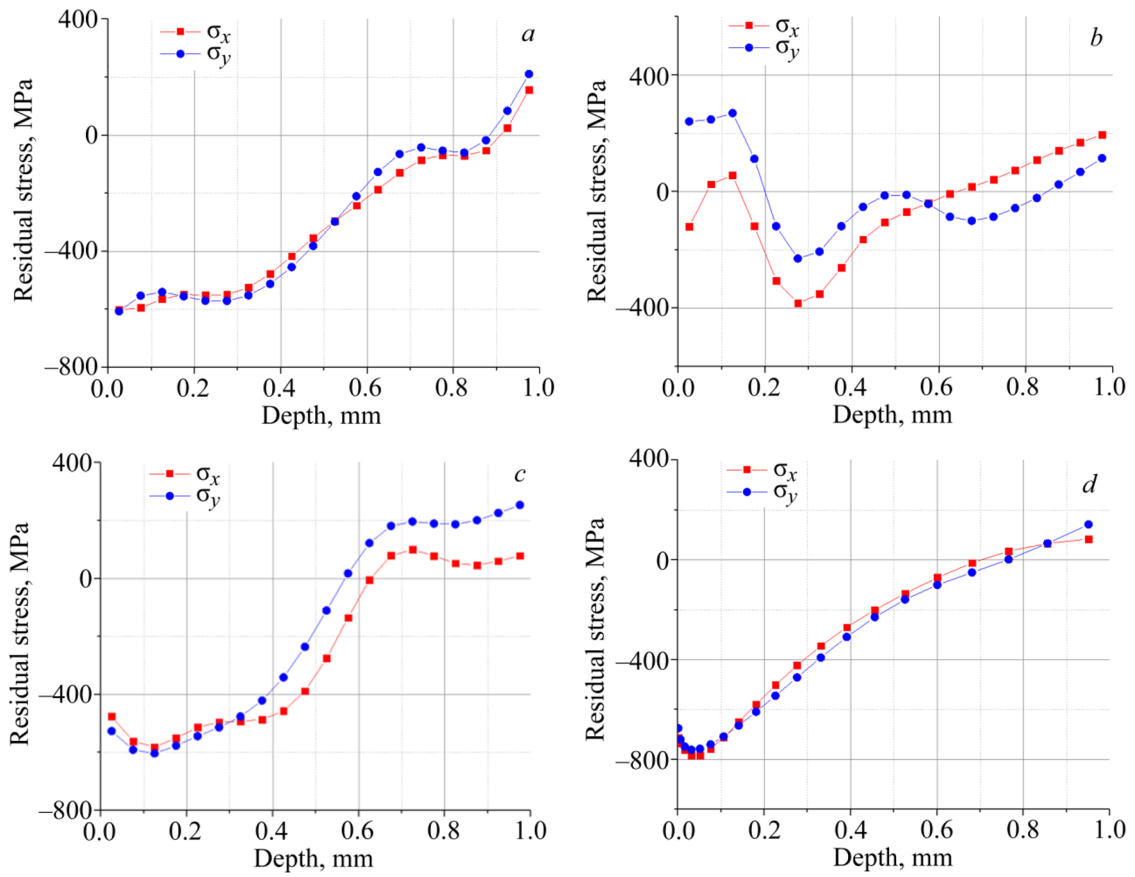


Fig. 2. Dependences of the RSs on the layer depths in the samples after LSP treatment in modes 1 (a), 2 (b), 3 (c), and 4 (d).

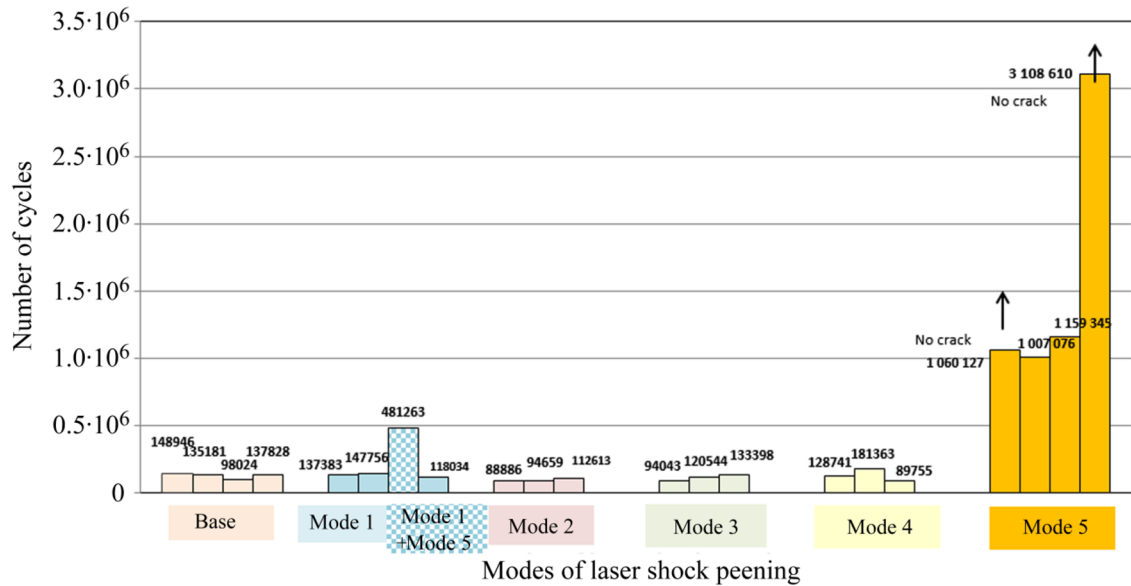


Fig. 3. Results of the fatigue tests of the Ti64 alloy specimens without treatment and after LSP in modes 1–5.

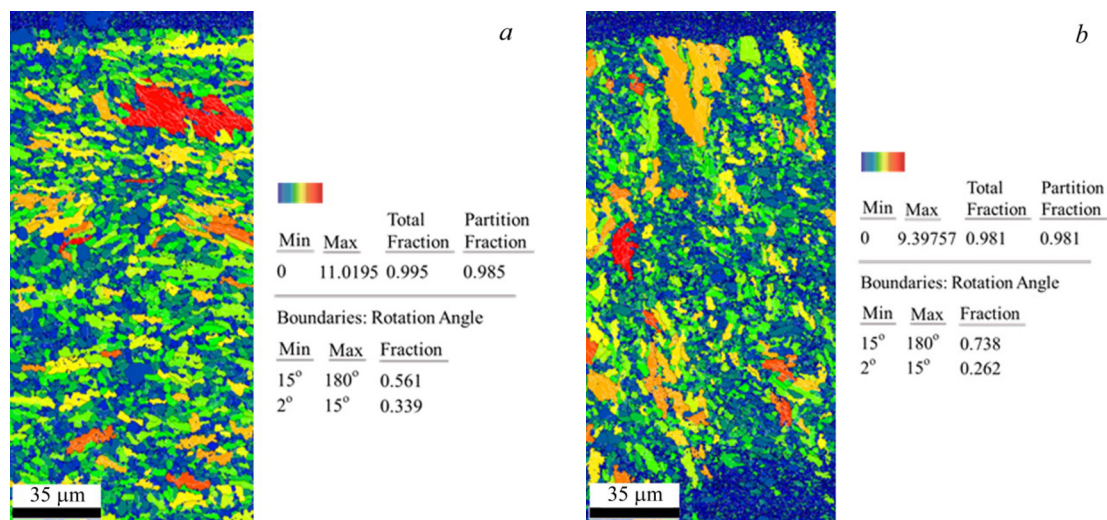


Fig. 4. Map of the grain orientation spread (GOS) of the Ti64 alloy specimen treated in modes 4 (a) and 5 (b).

Thus, modes 1–4 of LSP treatment of the specimen surface do not provide a significant increase in the fatigue life compared to the reference samples without treatment. Modification of mode 1 to *mode 1 + mode 5* made it possible to increase the resource by about 4 times, but the sample treatment area and accordingly, the treatment time increased. At the same time, after the LSP treatment of only the edge of the specimen inside the round notch (mode 5), the fatigue life demonstrated at least sevenfold increase compared to the reference specimens without treatment. From the viewpoint of increasing the fatigue life of the flat Ti64 alloy specimens, the LSP treatment mode 5 is the most effective.

## STRUCTURAL STUDIES

After LSP, the grains had an elongated shape and a pronounced texture. From the grain orientation spread (GOS) and kernel average misorientation (KAM) maps, it was found that the grains were strongly deformed. The presence of grains with high GOS values in the near-surface zones indicates an increased number of defects, which is also confirmed by the KAM maps. The results of structural studies of the most efficient treatment modes 4 and 5 are presented below. When analyzing the microstructure of a specimen treated in mode 4, a significant increase in the LSP impact depth was observed. The hardened grains were detected at least at a depth of 200 μm (Fig. 4a). The dislocation density increased at depths up to 200 μm (Fig. 5a). In addition, the shape of the grains in the surface layer became closer to the equiaxed one.

From our analysis of the microstructure maps of the samples after LSP in mode 5, it follows that a change in the predominant grain orientation significantly affects the laser impact depth. On the GOS maps, the grains with increased defect contents are found at depths up to 1 000 μm (Fig. 4b). A similar result is also shown in the KAM maps (Fig. 5b). On these maps, the LSP treatment is directed from top to bottom. From our analysis of the specimen microstructure, it follows that after the LSP treatment, the grain misorientation changes, and the number of grains with increased defect contents increases. These changes correlate with the level and depth of the compressive residual stresses caused by the LSP treatment.

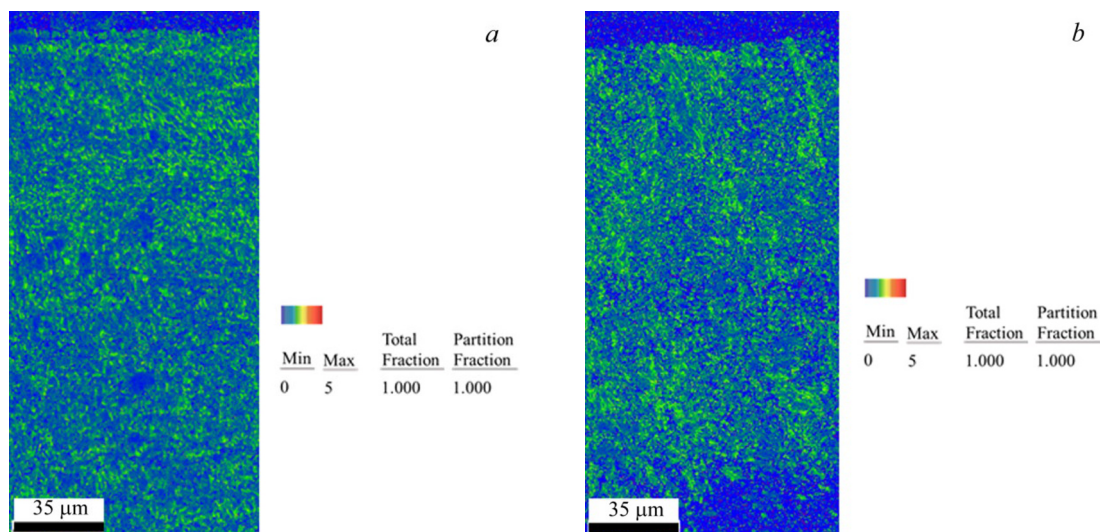


Fig. 5. Map of the kernel average misorientation (KAM) of the Ti64 alloy specimen treated in modes 4 (a) and 5 (b).

## CONCLUSIONS

The data on the effect of different LSP treatment modes on the fatigue properties and structure of titanium specimens with a concentrator have been obtained. It was shown that, along with the treatment mode, the treatment position on the sample surface plays the significant role. For the flat Ti64 alloy specimens with the circular notch, the most effective mode in terms of improving the fatigue life is the LSP treatment of the edge face inside the circular notch rather than the treatment of the flat specimen surface. The samples treated in this mode have improved the fatigue life by about 8 times compared to the specimens without treatment.

The comprehensive analysis of the data on the RS values and microstructural changes associated with the RS formation during LSP in various modes has been carried out that showed a correlation between the compressive RS layer depth and the depth of detection of grains with strong misorientations. Thus, mode 4 of the LSP treatment during which the RS profile was formed with the maximum compressive RS of 800 MPa at a depth of 200  $\mu\text{m}$  and the maximum depth of the compressive RS detection (up to 800  $\mu\text{m}$ ), the increased dislocation densities were observed in the microstructure of the material at depths up to 200  $\mu\text{m}$  and the change in the grain shapes that became more equated. The greatest laser impact effect on the material microstructure was found for the specimens after the LSP treatment in mode 5, which made it possible to significantly increase the fatigue life. The grains with increased defect contents were observed at depths up to 1 000  $\mu\text{m}$ , and the grain shapes changed.

Thus, the LSP treatment modes in which it is possible to achieve the significant increase in the fatigue life of the flat Ti64 alloy specimens with the round notch were found. The RS profiles obtained after different LSP treatment modes and the microstructural studies suggest that exactly changes in the structure are responsible for the residual stress field formation.



## COMPLIANCE WITH ETHICAL STANDARDS

### Author contributions

A.N.V. and E.A.G. carried out the experiment; A.N.V. wrote the manuscript with support from A.Y.I. and E.A.G.; A.Y.I. helped supervise the project; O.A.P. supervised the project. All authors have read and agreed to the published version of the manuscript.

### Conflicts of interest

The authors declare that they have no known competing financial interests or personal relationships that could have appeared to influence the work reported in this paper.

### Funding

The structural studies were carried out within the framework of the Government Assignment (Registration No. 20-48-596005). The laser shock peening and the fatigue tests were supported by the Russian Science Foundation (Project No. 22-79-10168; <https://rscf.ru/project/22-79-10168/>).

### Financial interests

The authors have no relevant financial or non-financial interests to disclose.

### Institutional review board statement

Applicable.

## REFERENCES

1. G.A. Askaryan, E.M. Moroz, *J. Exp. Theor. Phys.*, **43**, 2319–2320 (1962).
2. R. Sundar, P. Ganesh, R. K. Gupta, *et al.*, *Lasers Manuf. Mater. Proc.*, **6**, 424–463 (2019); <https://link.springer.com/article/10.1007/s40516-019-00098-8>.
3. P. Ganesh, R. Sundar, H. Kumar, *et al.*, *Opt. Lasers Eng.*, **50**, 678–686 (2012); <https://doi.org/10.1016/j.optlaseng.2011.11.013>.
4. P. Ganesh, R. Sundar, H. Kumar, *et al.*, *Mater. Des.*, **54**, 734–741 (2014); <https://doi.org/10.1016/j.matdes.2013.08.104>.
5. B. K. Pant, R. Sundar, H. Kumar, *et al.*, *Mater. Sci. Eng. A*, **587**, 352–358 (2013); <https://doi.org/10.1016/j.msea.2013.08.074>.
6. R. K. Gupta, R. Sundar, B. S. Kumar, *et al.*, *J. Mater. Eng. Perform.*, **24**, 2569–2576 (2015); <http://doi.org/10.1007/s11665-015-1530-1>.
7. R. Sundar, P. Ganesh, B. S. Kumar, *et al.*, *J. Mater. Eng. Perform.*, **25**, 3710–3724 (2016); <https://doi.org/10.1007/s11665-016-2220-3>.
8. R. K. Gupta, B. S. Kumar, R. Sundar, *et al.*, *Corros. Eng. Sci. Tech.*, **52**, No. 3, 220–225 (2017); <https://doi.org/10.1080/1478422X.2016.1254422>.
9. A. A. Shaniavski and G. V. Skvortsov, *FFEMS*, **22**, No. 7, 609–619 (1999); [https://doi.org/10.1016/S0266-538\(98\)00105-5](https://doi.org/10.1016/S0266-538(98)00105-5).



10. A. Umapathi and S. Swaroop, *Opt. Laser Technol.*, **119**, 105568 (2019); <https://doi.org/10.1016/j.optlastec.2019.105568>.
11. H. Chen, Y. Guan, L. Zhu, *et al.*, *Mater. Chem. Phys.*, **259**, 124025 (2021); <https://doi.org/10.1016/j.matchemphys.2020.124025>.
12. J. Zhao, Y. Dong, and C. Ye, *Int. J. Fatigue*, **100**, 407–417 (2017); <https://doi.org/10.1016/j.ijfatigue.2017.04.002>.
13. R. Sunab, S. Keller, Y. Zhuc, *et al.*, *Int. J. Fatigue*, **145**, 106081 (2021); <https://doi.org/10.1016/j.ijfatigue.2020.106081>.
14. D. C. van Aswegen and C. Polese, *Int. J. Fatigue*, **142**, 105969 (2021); <https://doi.org/10.1016/j.ijfatigue.2020.105969>.
15. S. N. van Staden, C. Polese, D. Glaser, *et al.*, *MRP*, **4**, 117–122 (2018); <http://doi.org/10.21741/9781945291678-18>.
16. G. A. Hartman and D. A. Johnson, *Exp. Mech.*, **27**, No. 1, 106–12 (1987); <https://doi.org/10.1007/BF02318872>.